Journal of Molecular Catalysis A: Chemical 315 (2010) 226–230

Contents lists available at ScienceDirect

Journal of Molecular Catalysis A: Chemical

journal homepage: www.elsevier.com/locate/molcata

Size-dependent heterogeneous catalytic kinetics

Dmitry Yu. Murzin

Åbo Akademi University, Turku/Åbo, Finland

ARTICLE INFO

Article history:
Received 6 May 2009
Received in revised form
21 September 2009
Accepted 27 September 2009
Available online 3 October 2009

Keywords:
Nanocatalysis
Thermodynamics
Kinetics

ABSTRACT

A quantitative thermodynamic approach is considered with the aim to describe the size-dependent Langmuir–Hinshelwood mechanism and the two-step catalytic cycle. The general treatment takes into account surface energy excess due to an intrinsic increase in chemical potential with size decrease as well as the changes in chemical potential upon adsorption. Numerical simulations as well as qualitative analysis show that for catalytic reactions over nanoparticles not only the rates but also reaction orders can vary depending on the size of nanoclusters. Comparison with experimental data is given.

1. Introduction

Heterogeneous catalytic kinetics is an established field of research not only in academia but also in industry, since kinetic models are routinely applied to modeling of large scale industrial reactors.

Progress in physical methods of nanomaterials characterization, and computational methods as well as a discovery of remarkable reactivity of specifically designed nanoparticles (e.g. gold) resulted in the revival of the interest to the problem of structure sensitivity, i.e. dependence of the rate on particle size [1–5]. Such variations are observed typically in the domain of 2–20 nm.

The dependence of turnover frequency per exposed (i.e. available for catalysis) site as a function of the nanoparticle dimension is given in Fig. 1.

It should be noted that structure sensitivity is a complex phenomenon [6]. Explanation of this phenomenon on a mechanistic level might involve quantum size effects, metastability nano-structures under reactions conditions, defect sites, and metal–support interface chemistry as well as other geometric (ratio of sites with different coordination environment), electronic (ionization potential, binding energies) or steric (changes in adsorption mode with crystal size) properties. In addition particle size effects in heterogeneous catalyzed reactions of e.g. hydrocarbons could be related to carbon deposition [7].

Size-dependent kinetics addressed on a quantitative level is very rarely described in the literature. It is interesting to note that size-dependent adsorption of nanocrystal surfaces was recently discussed [8–11].

An explanation for size-dependent adsorption utilized in Refs. [8–11] was based on the application of Laplace–Young equation, which takes into account changes in the interface free energy, namely an increase in the chemical potential of the active phase due to excessive surface energy and an increase in the internal Laplacian pressure with particle size decrease. According to the model [11] the equilibrium adsorption constant increases as material size decreases, which is in agreement with the experimental data [8] of adsorption of some organic acids on anatase.

Thermodynamic analysis of the nanoparticle size effect on adsorption equilibrium and rates was performed in Ref. [12]. This type of approach to catalytic kinetics, when the rate is governed by adsorption, can explain only a decrease in turnover frequency with the particle size increase.

In order to explain another type of behavior, i.e. TOF increase for large particle size, which corresponds to the occurrence of rate (per mass) maximum, a concept of an increase in chemical potential upon adsorption with crystal size increase was utilized in Ref. [13] without, however, explicit discussion about the differences in these two approaches. Two-step and Christiansen sequences, as well as Langmuir–Hinshelwood mechanisms were considered [13], showing that for catalytic reactions over nanoparticles not only the rates but also reaction orders can be different from those obtained for large nanoclusters. Comparison with experimental data for Fischer–Tropsch synthesis by cobalt supported on carbon nanofibers, as well as for crotonaldehyde hydrogenation over gold supported on TiO_2 was utilized for illustrating applicability of the thermodynamic analysis for the explanation of nanoparticle size effect on kinetics.

E-mail address: dmurzin@abo.fi.

1381-1169/$ – see front matter © 2009 Elsevier B.V. All rights reserved.
doi:10.1016/j.molcata.2009.09.016

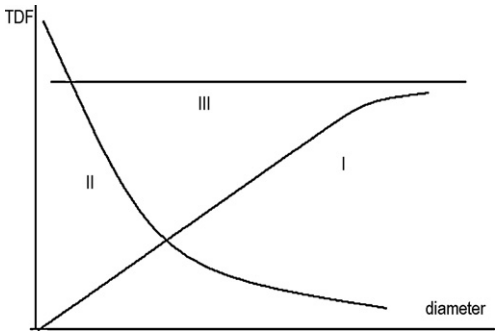

Fig. 1. Structure sensitivity plots.

In the present communication a treatment generalizing previous considerations [13] is considered with an explicit discussion on the differences between intrinsic and induced surface energy excess.

2. Thermodynamics

The chemical potential $\mu_i(r)$ of a substance i differs from the bulk value μ_∞ depending of the radius r [12]

$$\mu_i(r) = \mu_\infty + \delta_{\text{int}}(r) \tag{1}$$

where δ_{int} is the intrinsic chemical potential increment due to excessive surface energy.

In the simplest treatment the chemical potential increment is inversely proportional to the particle radius [12,14]

$$\delta_{\text{int}}(r) = \frac{\delta'_{\text{int}}}{r} \tag{2}$$

where δ'_{int} is the size-independent term in intrinsic chemical potential increment, whose value according to Ref. [12] is twice as high as σV_m, the latter being the surface tension and the partial molar volume of the substance forming the condensed phase, respectively. Note that the surface tension of metals is within a range of 1–2 J/m^2, while the molar volume of catalytically active metals is within a range of 6–10 cm^3/mol.

The corresponding change in the Gibbs energy upon adsorption is given by

$$\Delta G_{ads,\infty} = \Delta G_{ads}(r) + \delta_{\text{int}} \tag{3}$$

Since $\Delta G_{ads}(r) < 0$ and δ_{int} is positive, the absolute value of $\Delta G_{ads,\infty}$ is lower than that of $\Delta G_{ads}(r)$. Such a case, discussed in Ref. [12], can be graphically visualized as in Fig. 2a. This figure is based on an assumption that the excess of surface energy is relaxed upon adsorption. The corresponding equation for adsorption kinetics was derived in Ref. [12].

Keeping in mind that

$$\Delta G_r = -RT \ln K_r; \qquad \Delta G_\infty = -RT \ln K_\infty \tag{4}$$

the following equation can be easily obtained:

$$K_r = K_\infty \exp\left(\frac{\delta_{\text{int}}}{RT}\right) = K_\infty \exp\left(\frac{\delta'_{\text{int}}}{rRT}\right) \tag{5}$$

Such dependence implies lower adsorption constant for larger particles in agreement with experimental data [8].

Making use of the relationship between thermodynamics and kinetics expressed by Brønsted equation $k = gK^\alpha$ [15], where k is the rate constant, K is the equilibrium constant, g and α (Polanyi parameter, typically equal to 0.5) are values, constant for a series of reactions compared, it can be concluded that for larger particles lower adsorption rate should be obtained explaining the decrease in TOF with particle size, if the rate is determined by adsorption.

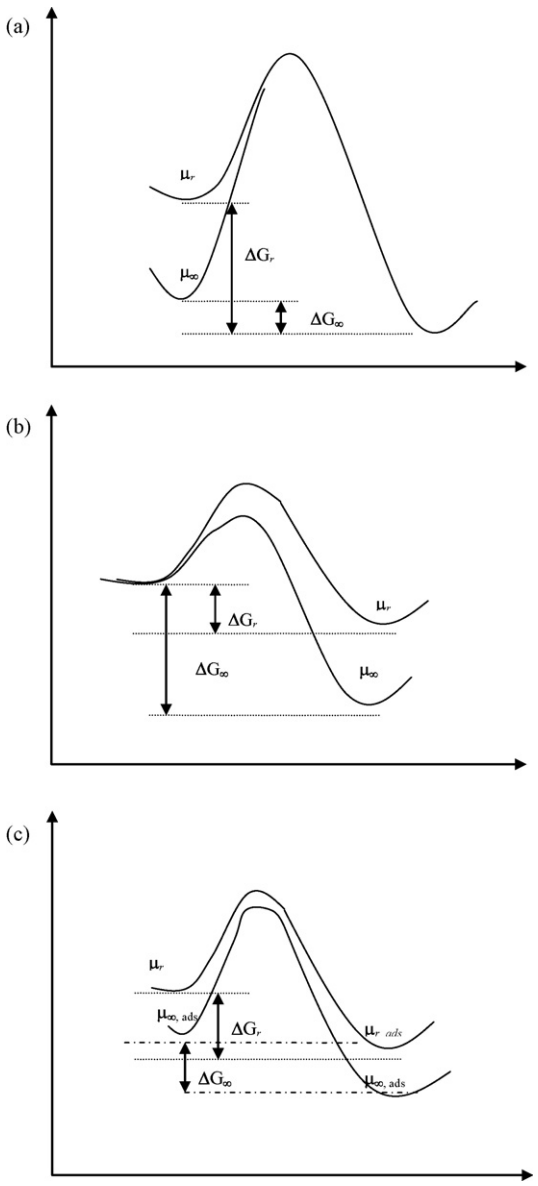

Fig. 2. Potential energy diagrams for adsorption in case of (a) intrinsic stress, (b) induced stress, and (c) combination of induced and intrinsic stress.

Studies of the adsorption processes in porous materials showed that adsorbent is not inert, since the deformation of the solid can occur [16,17]. A somewhat similar concept was utilized [18] for studies of adsorption of organic molecules on platinum nanoclusters when the surface distortion energy, i.e. the energy difference between the optimized clean surface and the optimized surface structure upon adsorption was taken into account. Deformation of nanoclusters [18] or porous solids [16,17] was considered to be elastic, meaning that the surface free energy can be restored to its bulk value when there is no stress imposed by adsorbed species. It implies that

$$\mu_j(r)_{ads} = \mu_{\infty,j,ads} + \delta_{ext}(r) \tag{6}$$

where $\mu_j(r)_{ads}$ is the chemical potential of an adsorbed substance j, which depends on the radius r, $\mu_{\infty,j,ads}$ is the corresponding bulk value, δ_{ext} is the external (induced) chemical potential increment upon adsorption.

The corresponding change in the Gibbs energy is expressed by

$$\Delta G_{ads,\infty} = \Delta G_{ads}(r) - \delta_{ext}(r) \tag{7}$$

Following the same reasoning as above for $\Delta G_{ads}(r) < 0$ and positive values of δ_{int}, the absolute value of $\Delta G_{ads,\infty}$ is larger than that of $\Delta G_{ads}(r)$. Such approach, visualized by Fig. 2b, was utilized [13] for thermodynamic analysis of adsorption and catalytic kinetics. This assumption leads to larger adsorption constant and higher adsorption rate for larger particles. It is interesting to note that larger values of adsorption constants were detected [8] for adsorption of valeric acid on anatase in the case of significant increase in the concentration of this acid.

The more general case is presented in Fig. 2c and takes into account both intrinsic (i.e. excess of surface energy with particle size increase) and induced (i.e. excess of surface energy due to external stress exerted by adsorbed molecules) changes in the chemical potential, leading finally to

$$\Delta G_{ads,\infty} = \Delta G_{ads}(r) + \delta_{int}(r) - \delta_{ext}(r) = \Delta G_{ads}(r) + \Delta\delta(r) = \Delta G_{ads}(r) + \frac{\Delta\delta'}{r} \quad (8)$$

Note that the values of $\Delta\delta(r)$ could be either positive or negative depending on which type of surface energy excess is dominating, internal or external.

3. Reaction sequences

Let us now consider the two-step mechanism with two kinetically significant steps [19,20], which implies that one of the several surface intermediates is the most abundant, while all the others are present on the surface at much inferior concentration levels:

$$\begin{array}{l} 1.\ Z + A_1 \leftrightarrow ZI + B_1 \\ 2.\ \underline{ZI + A_2 \leftrightarrow Z + B_2} \\ A_1 + A_2 \leftrightarrow B_1 + B_2 \end{array} \quad (9)$$

where A_1 and A_2 are reactants, B_1 and B_2 are products, Z is the surface site and I is an adsorbed intermediate.

The rate of the reaction in the case of ideal surfaces under steady-state conditions (v) is given by [21–23]

$$v = \frac{k_1 P_{A_1} k_2 P_{A_2} - k_{-1} P_{B_1} k_{-2} P_{B_2}}{k_1 P_{A_1} + k_2 P_{A_2} + k_{-1} P_{B_1} + k_{-2} P_{B_2}} = \frac{\omega_1\omega_2 - \omega_{-1}\omega_{-2}}{\omega_1 + \omega_2 + \omega_{-1} + \omega_{-2}} \quad (10)$$

where P_{A_1}, etc. are partial pressures (for gas-phase reactions) or concentrations (for liquid-phase reactions), k_i – kinetic constants, and ω_i – frequencies of steps (i.e. $\omega_1 = k_1 P_{A_1}$, etc.).

It follows from the previous considerations (Eqs. (1)–(4) and Brønsted equation) that the rates constants for the first step are

$$k_1(r) = k_1 e^{\alpha_1 \Delta\delta'/r}; \qquad k_{-1}(r) = k_{-1} e^{(\alpha_1 - 1)\Delta\delta'/r} \quad (11)$$

where α is the Polanyi parameter.

Since the overall Gibbs energy for the two-step sequence does not change in the presence of a catalyst $\Delta G = \Delta G_1 + \Delta G_2$, it holds for the second step

$$k_2(r) = k_2 e^{(\alpha_2 - 1)\Delta\delta'/r}; \qquad k_{-2}(r) = k_{-2} e^{-\alpha_2 \Delta\delta'/r} \quad (12)$$

Finally the following rate expression can be obtained:

$$v(r) = \frac{(k_1 P_{A_1} k_2 P_{A_2} - k_{-1} P_{B_1} k_{-2} P_{B_2}) e^{(\alpha_2 + \alpha_1 - 1)\Delta\delta'/r}}{k_1 P_{A_1} e^{\alpha_1 \Delta\delta'/r} + k_2 P_{A_2} e^{(\alpha_2 - 1)\Delta\delta'/r} + k_{-1} P_{B_1} e^{(\alpha_1 - 1)\Delta\delta'/r} + k_{-2} P_{B_2} k_{-2} e^{\alpha_2 \Delta\delta'/r}} \quad (13)$$

For the sake of clarity in order to demonstrate the influence of the size of clusters on the reaction rate it can be assumed following Ref. [19] that $\alpha_1 = \alpha_2 = \alpha$.

$$v(r) = \frac{(k_1 k_2 P_{A_1} P_{A_2} - k_{-1} k_{-2} P_{B_1} P_{B_2}) e^{(2\alpha - 1)\Delta\delta'/r}}{(k_1 P_{A_1} + k_{-2} P_{B_2}) e^{\alpha\Delta\delta'/r} + (k_2 P_{A_2} + k_{-1} P_{B_1}) e^{(\alpha - 1)\Delta\delta'/r}} \quad (14)$$

Neglecting the impact of the reverse reaction by assuming that one of the steps is irreversible ($k_{-2} \approx 0$) one arrives at

$$v(r) = \frac{\omega_2 e^{(\alpha - 1)\Delta\delta'/r}}{1 + ((\omega_2 + \omega_{-1})/\omega_1) e^{-\Delta\delta'/r}} \quad (15)$$

It should be noted that the Eley–Rideal mechanism can be treated as a special case of two-step sequence [13].

Besides two-step sequence, rather often the Langmuir–Hinshelwood mechanism is applied

$$\begin{array}{l} 1.\ A_{(g)} + Z = ZA_{(ads)} \text{(quasi-equilibrium)} \\ 2.\ B_{(g)} + Z = ZB_{(ads)} \text{(quasi-equilibrium)} \\ 3.\ \underline{ZA_{(ads)} + ZB_{(ads)} \Rightarrow C_{(g)} + 2Z} \\ A + B \rightarrow C \end{array} \quad (16)$$

where the surface reaction between the two adsorbed species is considered to be the rate-determining step.

The reaction rate is expressed by

$$v = \frac{k_3 K_1 P_A K_2 P_B}{(1 + K_A P_1 + K_2 P_B)^2} \quad (17)$$

Similarly to Eq. (5), the following equations could be written:

$$K_{1,r} = K_{1,\infty} e^{\Delta\delta'/r}; \qquad K_{2,r} = K_{2,\infty} e^{\Delta\delta'/r} \quad (18)$$

The Gibbs energy of the third step in mechanism (16) should follow:

$$\Delta G_{3,\infty} = \Delta G_3(r) - 2\Delta\delta \quad (19)$$

Resulting in ($\alpha_3 = \alpha$)

$$k_3(r) = k_3 e^{(2\alpha - 2)\Delta\delta'/r} \quad (20)$$

and leading finally to

$$v(r) = \frac{k_3 K_1 P_A K_2 P_B e^{2\alpha\Delta\delta'/r}}{(1 + (K_A P_1 + K_2 P_B) e^{\Delta\delta'/r})^2} \quad (21)$$

which together with Eq. (14) will be utilized below for an analysis of the nanoparticle size effect on kinetics. These equations express the reaction rate per unit of surface (mol/s m^2) while often experimental data are reported per unit of catalyst weight, which implies that [12]

$$V(r) = S'(r) v(r) = \frac{4\pi r^2}{4/3\pi r^3 \rho} = \frac{3}{r\rho} \quad (22)$$

where specific surface area $S'(r)$ is in m^2/g, and ρ is the density of catalytic phase.

4. Dependence of kinetic regularities on the particle size

Rearranging Eq. (15) and taking into account (22) one arrives at

$$V(r) = \frac{\omega_1\omega_2 e^{(2\alpha - 1)\Delta\delta'/r}}{\omega_1 e^{\alpha\eta/r} + (\omega_2 + \omega_{-1}) e^{(\alpha - 1)\Delta\delta'/r}} \frac{3}{r\rho} \quad (23)$$

and

$$V(r) = \frac{\omega_2 e^{(\alpha - 1)\Delta\delta'/r}}{1 + ((\omega_2 + \omega_{-1})/\omega_1) e^{-\Delta\delta'/r}} \frac{3}{r\rho} = \frac{p_1 e^{(\alpha - 1)\Delta\delta'/r}}{1 + p_2 e^{-\Delta\delta'/r}} \frac{1}{r} \quad (24)$$

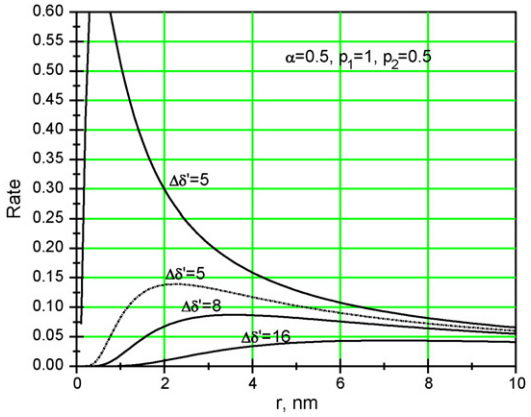

Fig. 3. Dependence of reaction rate on the cluster size for the two-step sequence (Eq. (24)) at different values of $\Delta\delta'$ ($\alpha = 0.5$, $p_1 = 1$, $p_2 = 0.5$).

In the case of $\Delta\delta' > 0$ for large values of the nanoparticle size $\omega_1 e^{\alpha\Delta\delta'/r} \ll (\omega_2 + \omega_{-1})e^{(\alpha-1)\Delta\delta'/r}$, which gives a first order in reactant A_1. If in addition $\omega_2 \gg \omega_{-1}$ a zero order with respect to A_2 is observed. On the contrary, when the size of clusters is small, it follows from Eq. (23) that $\omega_1 e^{\alpha\Delta\delta'/r} \gg (\omega_2 + \omega_{-1})e^{(\alpha-1)\Delta\delta'/r}$, i.e. a zero order in A_1 and a first order in reactant A_2 (when $\omega_2 \gg \omega_{-1}$).

Numerical simulations for the two-step sequences (i.e. Eq. (24)) are given in Fig. 3 for some values of parameters, showing that at high values of parameter $\Delta\delta'$ the influence of the nanoparticle size is less pronounced. The absolute values of the cluster size at which maxima are observed are in the region of 2–4 nm in line with experimental observations.

For the Langmuir–Hinshelwood mechanism when $\Delta\delta' > 0$ and reaction is carried out on large particles, it holds that $1 \gg (K_A P_1 + K_2 P_B)e^{\Delta\delta'/r}$ and the reaction rate displays the first order in both reactants with TOF diminishing as size increases. On small particles the rate is given by

$$v(r) = \frac{k_3 K_1 P_A K_2 P_B}{(K_A P_1 + K_2 P_B)^2} \tag{25}$$

which shows independence of turnover frequency with the size as well as a fractional order or even negative orders in reactants.

Numerical analysis for Langmuir–Hinshelwood kinetic equation:

$$V(r) = \frac{k_3 K_1 P_A K_2 P_B e^{2\alpha\Delta\delta'/r}}{(1 + (K_A P_1 + K_2 P_B)e^{\Delta\delta'/r})^2} \frac{3}{r\rho} = \frac{p_1' e^{2\alpha\Delta\delta'/r}}{r(1 + p_2'' e^{\Delta\delta'/r})^2} \tag{26}$$

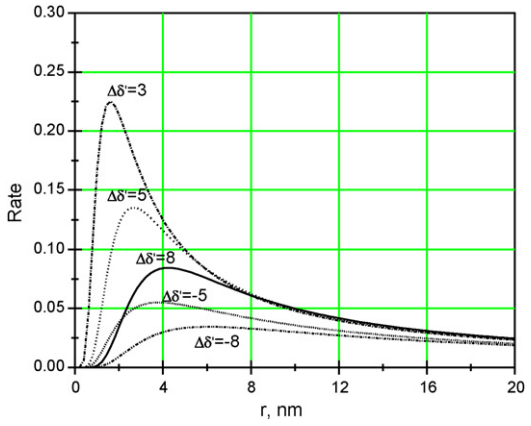

Fig. 4. Dependence of reaction rate on the cluster size at different values of $\Delta\delta'$ ($\alpha = 0.5$, $p'_1 = 1$, $p''_2 = 0.5$; Langmuir–Hinshelwood mechanism, Eq. (26)).

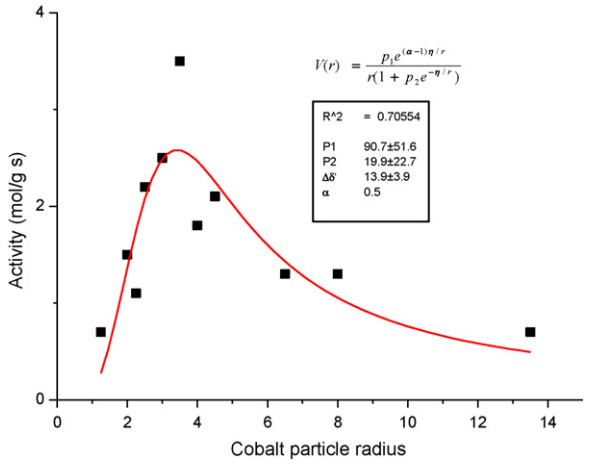

Fig. 5. Activity versus the average particle size for Fischer–Tropsch synthesis by cobalt supported on carbon nanofibers. Experimental data: squares [27] and calculations according to the two-step sequence.

is presented in Fig. 4. For the sake of comparison, analysis for negative values of $\Delta\delta'$ is given in this figure as well, demonstrating less pronounced dependence of the reaction rate on the nanoparticle size in the case of surface stress induced by adsorbed species.

According to Eq. (26) for positive values of $\Delta\delta'$ the reaction rate at low values of reactants partial pressures exhibits a decrease with increasing nanoparticle size.

5. Comparison with experimental data

Dependence showing rate maxima were reported for oxidation reactions over gold [24,25], hydrogenation of crotonaldehyde [26] and Fischer–Tropsch synthesis over cobalt supported on carbon nanofibers [27].

It was interesting to confirm if Eq. (24) could be used to explain the dependence of the reaction rate on the cobalt particle size [27]. For the numerical data fitting the value of Polanyi parameter was taken to be 0.5, which is often the case [22]. Fig. 5 demonstrates a good description of the experimental data.

The positive value of $\Delta\delta'$ follows from the numerical data fitting. It should be noted, however, that due to the structure of the model, having two steps, one of which could be considered as adsorption and another as desorption, an equally good fit (clearly with other values of kinetic parameters) can be achieved under the assumption of $\Delta\delta' < 0$, which in fact was demonstrated in Ref. [13]. These considerations indicate that the analysis of the nature of strain present in a catalytic system cannot be unequivocally done for a steady-state kinetics, unless the rate limiting step is adsorption or desorption. Data on adsorption kinetics as a function of the crystal size could serve as a basis for such discrimination.

More complicated dependence of thermodynamic functions on the size could be obtained for solid–fluid interface [28], following the original treatment of Tolman and Buff [29,30]. However, the "reasonable" [28] approximation of inverse dependence of potential increment on the crystal radius is probably sufficient for the purpose of kinetic modeling of particular catalytic reactions.

6. Conclusions

Concepts of surface thermodynamics, namely the surface energy excess, were used in the present treatment to explain structure-sensitive heterogeneous catalytic reactions. In the theoretical analysis intrinsic dependence of the chemical potential on nanocrystal size as well as the changes in chemical poten-

tial upon adsorption were considered. Size-dependent kinetic expressions were derived for the two-step catalytic cycle and Langmuir–Hinshelwood mechanism. Numerical simulations were carried out showing that not only the rates of heterogeneous catalytic reactions can exhibit maxima as a function of nanoparticle size but kinetic regularities could also vary. Experimental data of catalytic activity versus the average particle radius for Fischer–Tropsch synthesis by cobalt supported on carbon nanofibers showed good correspondence between the theory and experiments.

References

[1] A.T. Bell, Science 299 (2003) 1688.
[2] R. Schlögl, S.B. Abd, Hamid (Eds.), Angew. Chem. Int. Ed. 43 (2004) 1628.
[3] R. Narayanan, M.A. El-Sayed, Top. Catal. 47 (2008) 15.
[4] C.R. Henry, Appl. Surf. Sci. 164 (2000) 252.
[5] F. Klasovsky, P. Claus, in: B. Corain, G. Schmid, N. Toshima (Eds.), Metal Nanoclusters in Catalysis and Materials Science: The Issue of Size Control, Elsevier, Amsterdam, 2008, pp. 167–181.
[6] J. Rostrup-Nielsen, J. Catal. 27 (1972) 343.
[7] R.A. van Santen, Acc. Chem. Res. 42 (2009) 57.
[8] H. Zhang, R. Lee Penn, R.J. Hamers, J.F. Banfield, J. Phys. Chem. B 103 (1999) 4656.
[9] Q. Jiang, H.M. Lu, Surf. Sci. Rep. 63 (2008) 427.
[10] Q. Jiang, D.S. Zhao, M. Zhao, Acta Mater. 49 (2001) 3143.
[11] H.M. Lu, Z. Wen, Q. Jiang, Chem. Phys. 309 (2005) 303.
[12] V.N. Parmon, Doklady Phys. Chem. 413 (2007) 42.
[13] D.Yu. Murzin, Chem. Eng. Sci. 64 (1046) (2009) 64.
[14] A.I. Rusanov, Surf. Sci. Rep. 58 (2005) 111.
[15] J.N. Brønsted, Chem. Rev. 5 (1928) 231.
[16] A. Grosman, C. Ortega, Phys. Rev B 87 (2008) 085433.
[17] A. Grosman, C. Ortega, Langmuir 25 (2009) 8083.
[18] V. Nieminen, K. Honkala, A. Taskinen, D.Yu. Murzin, J. Phys. Chem. C 112 (2008) 6822.
[19] M.I. Temkin, Kinet. Katal. 25 (1984) 299.
[20] M. Boudart, K. Tamaru, Catal. Lett. 9 (1991) 15.
[21] M. Boudart, Kinetics of Chemical Processes, Prentice-Hall, Englewood Cliffs, NJ, 1968.
[22] M.I. Temkin, Adv. Catal. 28 (1979) 173.
[23] D.Yu. Murzin, T. Salmi, Catalytic Kinetics, Elsevier, 2005.
[24] G.J. Hutchings, M. Haruta, Appl. Catal. A Gen. 291 (2005) 2.
[25] M. Haruta, Chem. Rec. 3 (2003) 75.
[26] R. Zanella, C. Louis, S. Giorgio, R. Touroude, J. Catal. 223 (2004) 328.
[27] G.L. Bezemer, J.H. Bitter, H.P.C.E. Kuipers, H. Oosterbeek, J.E. Holewijn, X. Xu, F. Kapteijn, A.J. van Dillen, K.P. de Jong, J. Am. Chem. Soc. 128 (2006) 3956.
[28] Q. Jiang, H.X. Shi, M. Zhao, J. Chem. Phys. 111 (1999) 2176.
[29] R.C. Tolman, J. Chem. Phys. 17 (1949) 333.
[30] F.P. Buff, J. Chem. Phys. 19 (1951) 1591.